Applied Catalysis B: Environmental 100 (2010) 190–196

Contents lists available at ScienceDirect

Applied Catalysis B: Environmental

journal homepage: www.elsevier.com/locate/apcatb

Nano-silicon carbide supported catalysts for PEM fuel cells with high electrochemical stability and improved performance by addition of carbon

Haifeng Lv, Shichun Mu*, Niancai Cheng, Mu Pan

State Key Laboratory of Advanced Technology for Materials Synthesis and Processing, Wuhan University of Technology, Wuhan 430070, China

ARTICLE INFO

Article history:
Received 8 May 2010
Received in revised form 7 July 2010
Accepted 27 July 2010
Available online 4 August 2010

Keywords:
Silicon carbide
Support
Electrocatalyst
Stability
PEM fuel cell

ABSTRACT

Nano-silicon carbide was applied as a novel catalyst support in proton exchange membrane (PEM) fuel cells to improve catalyst stability, due to its excellent resistance to electrochemical oxidation. Homogeneously dispersed Pt nanoparticles were deposited on β-SiC (Pt/SiC) using an ethylene glycol reduction method. Furthermore, carbon was introduced into this Pt/SiC catalyst, (Pt/SiC/C), to improve its electrocatalytic performance by increasing the electrical conductivity. The electrochemical stability of SiC was investigated and showed almost no changes in the redox region after oxidation for 48 h at 1.20 V. Based on accelerated durability tests (ADT) and high-resolution transmission electron microscopy (HRTEM), the electrochemical stability of Pt/SiC/C was remarkably enhanced compared with the Pt/C catalysts, which could be attributed to the excellent stability of the SiC support and the addition of high electrical conductivity carbon.

1. Introduction

Attention has recently been focused on PEM fuel cells as both transportation and emergency electric power sources due to being environmentally friendly, having high power density, and low operating temperatures. However, insufficient stability of electrocatalysts remains a major obstacle to the widespread commercialization of this technology [1–3]. Currently, Pt or Pt-based alloys dispersed as nano-sized particulates on high surface area carbon, such as Vulcan XC-72, is the preferred electrocatalyst used in PEM fuel cells to obtain optimized catalytic activity at an acceptable cost.

In the state of art, carbon supports are susceptibly oxidized under chemical and electrochemical oxidation conditions at the fuel cell's cathode [4,5]. As carbon is corroded away, the noble metal nanoparticles will fall off from carbon support surfaces and aggregate into fewer, but much larger particles, resulting in a decrease of electrochemical surface area (ECSA). This results in reduced long-term performance of PEM fuel cells, making them inappropriate for most of the projected applications. Therefore, development of highly stable catalyst supports to enhance the stability of these catalysts is urgently desired [6].

Recently, ceramic materials have been considered as alternative support materials to replace the conventional carbon supports for fuel cell catalysts because of their unique mechanical properties, excellent thermal stability, and outstanding oxidation and acid corrosion resistance [7–9]. Haldar and coworkers [7] have reported that titanium nitride (TiN) nanoparticles acting as catalyst support material for PEM fuel cells showed higher catalytic performance, demonstrating the possibility of making a variety of Pt-based alloys with this class of transition metal-nitride or carbide ceramic materials as electrocatalysts for the PEM fuel cells. Our research group [8] has shown titanium diboride (TiB_2) as a catalyst support in PEM fuel cells, for the first time, where the stability of the Pt/TiB_2 catalyst is approximately four times better than that of the commercial Pt/C. However, TiB_2 powders used in this investigation have a relatively big particle size with less specific surface area and heavy density, which reduced the Pt utilization efficiency. Furthermore, Popov and coworkers [9] synthesized a novel TiO_2-supported Pt electrocatalyst and demonstrated that the synthesized Pt/TiO_2 electrocatalyst exhibited excellent fuel cell performance, as well as ultrahigh stability at high positive potentials. Despite the lower initial catalytic activity of the Pt/TiO_2 electrocatalyst, the low electrical conductivity of TiO_2 may prevent its use in fuel cells. Therefore, nano-sized ceramic and ceramic-based eletrocatalysts with higher catalytic activity are desired.

To our knowledge, no literature describes the use of nano-silicon carbide (SiC) as a catalyst support for noble metal in PEM fuel cells. SiC is a widely used material with many desirable properties, including high thermal conductivity, good mechanical resistance, and stability in acidic and oxidative environments [10–12]. For the first time, we report the synthesis of a Pt/SiC as PEM fuel cell electrocatalysts with homogeneously dispersed Pt nanoparticles supported on nano-SiC particles, and demonstrate the novel

* Corresponding author. Tel.: +86 27 87651837; fax: +86 27 87879468.
E-mail addresses: msc@whut.edu.cn, mushichun@gmail.com (S. Mu).

0926-3373/$ – see front matter © 2010 Elsevier B.V. All rights reserved.
doi:10.1016/j.apcatb.2010.07.030

carbon-mixed Pt/SiC electrocatalyst's excellent performance and electrochemical stability.

2. Experimental

2.1. Catalysts preparation

Polyol processes in ethylene glycol (EG) solution fabricated Pt/SiC catalysts as follows. To homogeneously deposit the Pt nanoparticles on the as-received β-SiC (Kaier Nano Co.), 120 mg of SiC was added to EG solution and ultrasonically treated for 30 min then transferred into a round bottom flask. Appropriate amounts of H_2PtCl_6 (Sinopharm Chemical Reagent Co., Ltd.) solution dropwised to SiC suspension under vigorous stirring, the pH scale of the mixture solution was adjusted to 12–13 by adding 2.0 M of NaOH aqueous solution, followed by refluxing the reaction mixture at 160 °C for 2–3 h to ensure complete reduction of the metal salts. The solution was stirred overnight at room temperature. After filtering and washing, the obtained catalyst was dried in a vacuum oven at 80 °C overnight. Reacted with sodium borohydride, no changes happened to the colorless and transparent filtrate, which demonstrated that all H_2PtCl_6 was reduced and deposited on SiC. The final catalyst obtained was denoted as Pt/SiC, where the Pt loading was maintained at 20 wt.%.

2.2. Catalyst characterizations

Microstructures of the as-received β-SiC support, as-prepared Pt/SiC, and the dispersion of Pt nanoparticles on SiC were characterized by JEOL 2010 high-resolution transmission electron microscopy (HRTEM).

For determination of the electrochemical performance and stability of supports and catalysts, a conventional three-electrode electrochemical cell was employed. All the electrochemical measurements were carried out in 0.5 M H_2SO_4 solution at 25 °C, and ultra-pure N_2 (Air Products) was passed through a H_2SO_4 solution for 30 min before the electrochemical measurements, a platinum electrode was the counter electrode, and a Hg/Hg_2SO_4 electrode was the reference electrode. For convenience, all potentials measured are referred to as the normal hydrogen electrode (NHE).

A polished glassy carbon disk electrode (3 mm diameter) was used as the substrate for the supported catalysts (or supports). The working electrode was fabricated as follows: 6 mg of the catalysts (or supports) was dispersed in 1 mL of deionized water and then mixed with 100 μL 5 wt.% perfluorosulfonic acid (PSFA) Nafion (Du Pont Co.) solution. The mixture was sonicated for 6 min to obtain an ink like slurry. 5 μL of this slurry was spread onto the flat surface of the glassy carbon disk using Finnpipette Digital Micropipette. For the carbon-mixed Pt/SiC catalysts (Pt/SiC/C), 6 mg of Pt/SiC and 1.5 mg of Vulcan XC-72 (Cabot Corporation) were mixed to prepare a working electrode in the same way.

Chronoamperometric and accelerated durability tests (ADT) were employed to investigate the electrochemical stability of both the supports and catalysts, which were widely applied to characterize electrochemical oxidation of supports and catalysts of PEM fuel cells [1,8,13]. In the chronoamperometric, a constant of 1.20 V was applied for 48 h in 150 ml solution. The ADT was conducted by cyclic voltammograms (CVs) between 0.6 and 1.20 V for 4000 cycles. Meanwhile, full-scale CVs from 0 to 1.20 V were recorded periodically before and after the chronoamperometric and ADT, where the constant scan rate was kept at 50 mV s^{-1}. The electrochemical surface area (ECSA) of catalysts was calculated with the charge of hydrogen adsorption peak as follows:

$$\mathrm{ECSA} = \frac{Q_H}{[\mathrm{Pt}] \times 0.21} \quad (1)$$

where [Pt] represents the platinum loading (mg cm^{-2}) in the electrode, Q_H is the charge for hydrogen adsorption (mC cm^{-2}) and 0.21 represents the charge required to oxidize a monolayer of H_2 on bright Pt [14]. The rotating disk electrode (RDE) curves were obtained in the scan range from 1.1 to 0.2 V, after oxygen bubbling for 30 min to characterize the oxygen reduction reaction (ORR) performance of the as-prepared catalysts.

3. Results and discussion

Fig. 1 shows the HRTEM images of as-received nano-β-SiC and homogeneously dispersed Pt nanoparticles supported on β-SiC. It can be seen that the β-SiC nanoparticles are uniform, and the average particle size is ~40 nm within the 30–50 nm range (shown in Fig. 1A). Fig. 1B–D demonstrates that Pt nanoparticles are successfully deposited and homogeneously dispersed on the novel supports with a particle size of ~3 nm. Fig. 1D shows that the crystal phases of Pt and β-SiC are identified by lattice analyses, the lattice spacing of Pt and β-SiC is ~0.19 and ~0.25 nm corresponding to Pt (2 0 0) and β-SiC (1 1 1), respectively. The inset shows the scheme of β-SiC structure. For comparison, HRTEM of the commercial 20 wt.% Pt/C (JM) is recorded (see Fig. 1E). It has been well established that dispersion of particles on supports and the metal particle size can strongly affect the catalytic activity of the catalyst [15,16]. The apparent similitude on the dispersion of Pt nanoparticles between Pt/SiC and Pt/C catalysts confirms high dispersion of Pt nanoparticles with a uniform particle size and no obvious aggregation is more easily achieved on SiC compared to TiB_2 ceramics [8], indicating that the introduced SiC as novel support of Pt nanoparticles is extraordinarily successful.

The CVs for Vulcan XC-72 and SiC ceramic after oxidation treatment at 1.20 V for different durations are plotted in Fig. 2. The applied potential of 1.20 V is selected in the experiments because the cathode potential of a PEM fuel cell is close to 1.20 V under open circuit conditions where the carbon support is very prone to oxidation [17]. It can be seen that the SiC ceramic has almost no change in the redox region after oxidation treatment for 48 h (Fig. 2A), which means there are negligible surface oxides. Contrarily, there are visible current peaks in the redox region for Vulcan XC-72, resulting from the surface oxide formation due to the hydroquinone-quinone (HQ-Q) redox couple on the carbon black surface [18]. Note that the current peak at about 0.60 V becomes stronger with treatment time and is accompanied by a general increase in capacitive current, which suggests a higher degree of surface carbon oxidation with potential-holding time. These results indicate that SiC is more resistant to electrochemical oxidation than Vulcan XC-72. Meanwhile, the concentration of Si ion in solution is ca. 0.09 μg ml^{-1} at 1.20 V for 48 h, identified by inductively coupled plasma atomic emission spectrometry (ICP-AES, PE), and the corrosion rate of Si in SiC is only ca. 0.28 μg h^{-1}, which resemble TiB_2 (0.2 μg h^{-1}) in previous studies [8]. This indicates that SiC is more corrosion resistant and durable when used in a fuel cell.

Next, the electrochemical performance of catalysts is evaluated. Typical hydrogen and oxygen adsorption and desorption behaviors (Fig. 3A) can be clearly detected on Pt/SiC and no additional current peak is seen, indicating that the SiC support is electrochemically inert and can be treated as a conductor in the potential region under PEM fuel cell conditions [7]. However, the low ECSA (13 m^2 g^{-1}) of Pt/SiC is not in accordance with the more homogeneous dispersion of Pt nanoparticles on the SiC, because of a low electrical conductivity of nanometer-scale ceramic material, which may prevent its use in fuel cells [9].

ADT of the Pt/SiC is carried out by continuously applying linear potential sweeps from 0.6 to 1.20 V, which accelerates dissolution and agglomeration of Pt nanoparticles, caused by surface

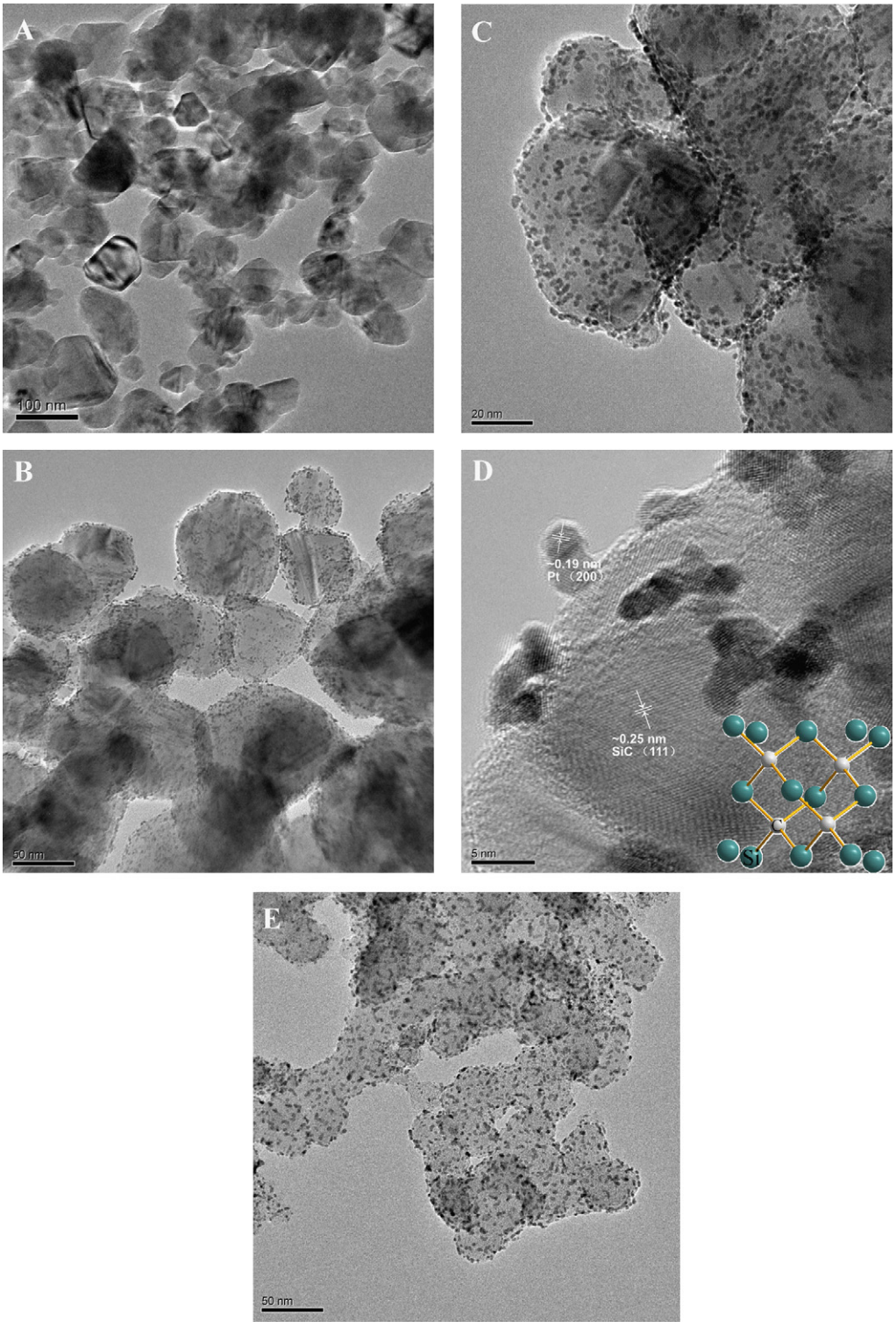

Fig. 1. HRTEM image of the SiC nanoparticles (A); HRTEM images of the Pt/SiC catalysts with different scale bars corresponding to 50 nm (B), 20 nm (C) and 5 nm (D); HRTEM image of the commercial 20 wt.% Pt/C catalysts (E).

oxidation/reduction cycles of Pt. Fig. 3B shows the changes of voltammograms versus the electrochemical oxidation cycle number. Surprisingly, no visible hydrogen adsorption and desorption peaks are observed for the Pt/SiC after 1000 cycles, implying that there is no catalytic activity for the Pt/SiC. At least three possibilities can account for such unexpected observation. The first possibility is that the corrosion of the SiC support at high positive potentials could result in a detachment of Pt nanoparticles from supports. In the above experiments, that SiC is more resistant to electrochemical oxidation than Vulcan XC-72 is demonstrated. In addition, Fig. 3C shows that the Pt nanoparticles are still highly dispersed on the SiC and the agglomeration of Pt particles is not found. Therefore, this hypothesis does not justify why there is no catalytic activity for the Pt/SiC after ADT. The second possibility is that nearly all the Pt nanoparticles could be dissolved in the electrolyte due to a weaker interaction between Pt nanaoparticles and the novel SiC support.

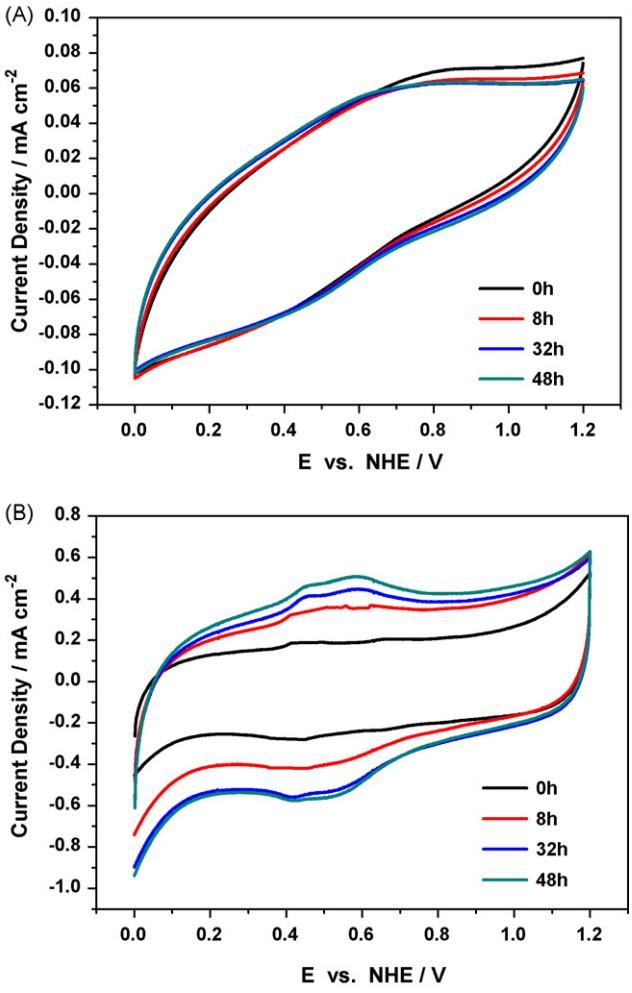

Fig. 2. CV curves of SiC (A) and carbon supports (Vulcan XC-72) (B) by held at 1.20 V for different durations (0.5 M H_2SO_4, scan rate: 50 mV s^{-1}).

This proposal can also be rejected by corresponding TEM images of the Pt/SiC after ADT as shown in Fig. 3C.

For the third possibility, electrical conductivity of the SiC support might decrease rapidly with the cycle number increment, which results in the catalytic activity of Pt/SiC entirely disappearing. Memming and coworkers [19] reported the electrochemical properties of silicon carbide and demonstrated that SiC was found leading to the formation of CO_2 and silicon oxides. The reaction equation can be written as:

$$SiC - 8e^- + 4H_2O \rightarrow SiO_2 + CO_2 + 8H^+ \quad (2)$$

In the case of the ADT, the SiC surface may be covered with a super thin insulating layer of silicon oxides as new supports of Pt nanoparticles, resulting in the decrease of the electrical conductivity of the support. However, although the formation of silicon oxides is so slow that we cannot detect reaction (2) in CV curves in Fig. 2A, it may affect the electrical conductivity of the SiC surface, leading to a low catalytic activity for the catalyst. Conditions vary in only CO_2 release during carbon corrosion, in this case, the formed super thin silicon oxide layer in surfaces of SiC is very stable, which could well explain no occurrence of agglomeration of Pt nanoparticles under ADT conditions (Fig. 3C).

To validate this hypothesis, an addition of carbon with superior electrical conductivity can be an effective solution to enhance the electron conduction and catalytic activity of catalysts. Therefore, the Pt/SiC/C catalyst is obtained by introducing 20 wt.% carbon

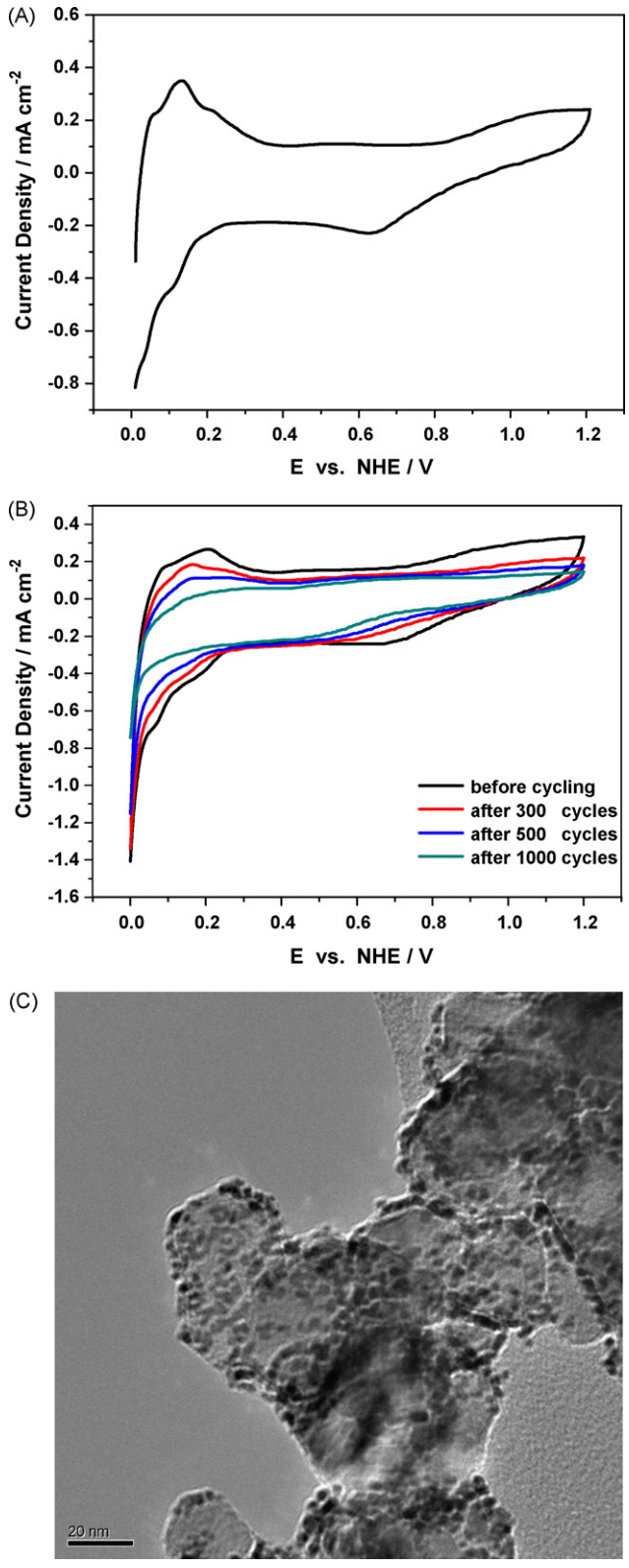

Fig. 3. CV curves of Pt/SiC catalysts (A); CV curves of Pt/SiC catalysts after ADT (B) (0.5 M H_2SO_4, scan rate: 50 mV s^{-1}) and HRTEM image of Pt/SiC after ADT (C).

(Vulcan XC-72) into Pt/SiC. The CV curves in Fig. 4A shows the ECSA (48 m^2 g^{-1}) of Pt/SiC/C is evidently increased compared with Pt/SiC (13 m^2 g^{-1}). The Pt/SiC/C shows a comparable ECSA with the Pt/C (62 m^2 g^{-1}). However, we believe that the ECSA could be further enhanced by using higher conductivity carbon or optimizing the proportion of carbon and Pt/SiC.

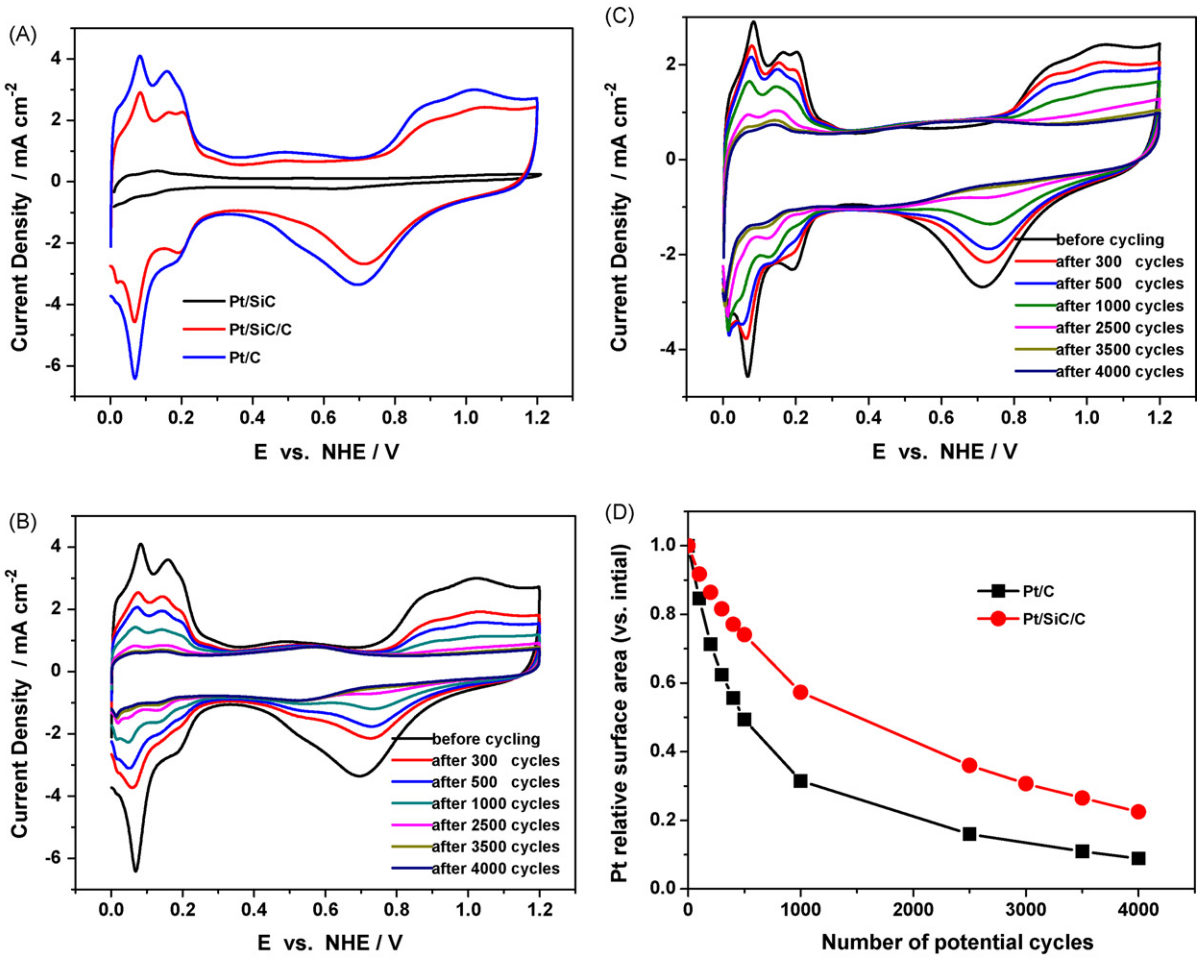

Fig. 4. Comparison of the CV curves of Pt/C, Pt/SiC/C and Pt/SiC (A); CV curves of Pt/C (B) and Pt/SiC/C (C) before and after ADT (0.5 M H_2SO_4, scan rate: 50 mV s^{-1}); changes of ECSA of catalysts related to Pt catalytic surface area with the increased potential cycles (D).

The ADT of both Pt/SiC/C and Pt/C catalysts is carried out by continuously applying linear potential sweeps. From Fig. 4B and C, both the catalysts exhibit a reduction in the hydrogen adsorption regions after the ADT, indicating a rapid decrease of ECSA with repeated potential cycling. Normalized with the initial one, the decrease of the ECSA is plotted as a function of cycle number in Fig. 4D. Surprisingly, after 1000 cycles the ECSA loss of Pt/C is 68.5%, whereas the Pt/SiC/C has only degraded 42.7%. It is evident that the degradation rate of the Pt/SiC/C is lower than that of the commercial Pt/C. Importantly, only 8.9% of the initial ECSA of Pt/C remains, whereas 22.5% of the initial ECSA for Pt/SiC/C remains after 4000 cycles, which clearly indicates that the new catalyst is significantly more stable compared with the commercial Pt/C under the same electrochemical acceleration condition. In addition, this result indicates that the third possibility as mentioned above is established.

The ORR is studied in oxygen-saturated electrolyte to evaluate the catalytic activity of the Pt/SiC/C electrocatalyst. On a RDE, the ORR activities of Pt/SiC/C and Pt/C measured with a scan rate of 10 mV s^{-1} at 1600 rpm (Fig. 5). The minor differences in the half-wave potential and diffusion limiting current of the catalysts indicate that they have similar ORR activity. Thus, the Pt nanoparticles of Pt/SiC/C retain their ORR activity for fuel cell catalysts. The ORR activity can be attributed to the higher utilization efficiency of Pt particles because of the homogeneous dispersion of Pt nanoparticles on the SiC and the influence of support materials [20,21]. Similar to SiC supports, our research group [8] and Haldar and coworkers [7] have demonstrated that TiB_2 and TiN supported Pt catalysts have an excellent activity of oxygen reduction in comparison with carbon-supported catalysts. Periodic measurement of ORR activity is also tested during the ADT. Fig. 5 shows the ORR curves of both the catalysts after 1000 cycles. The com-

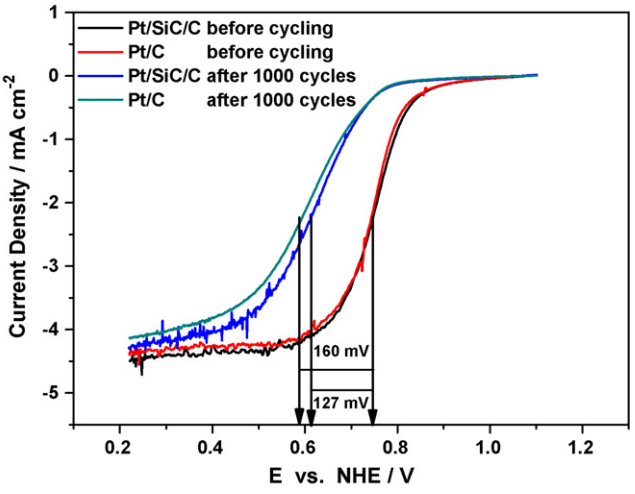

Fig. 5. Oxygen reduction reaction on the Pt/SiC/C and the commercial 20 wt.% Pt/C before and after 1000 cycles at 1600 rpm (0.5 M H_2SO_4, scan rate: 10 mV s^{-1}).

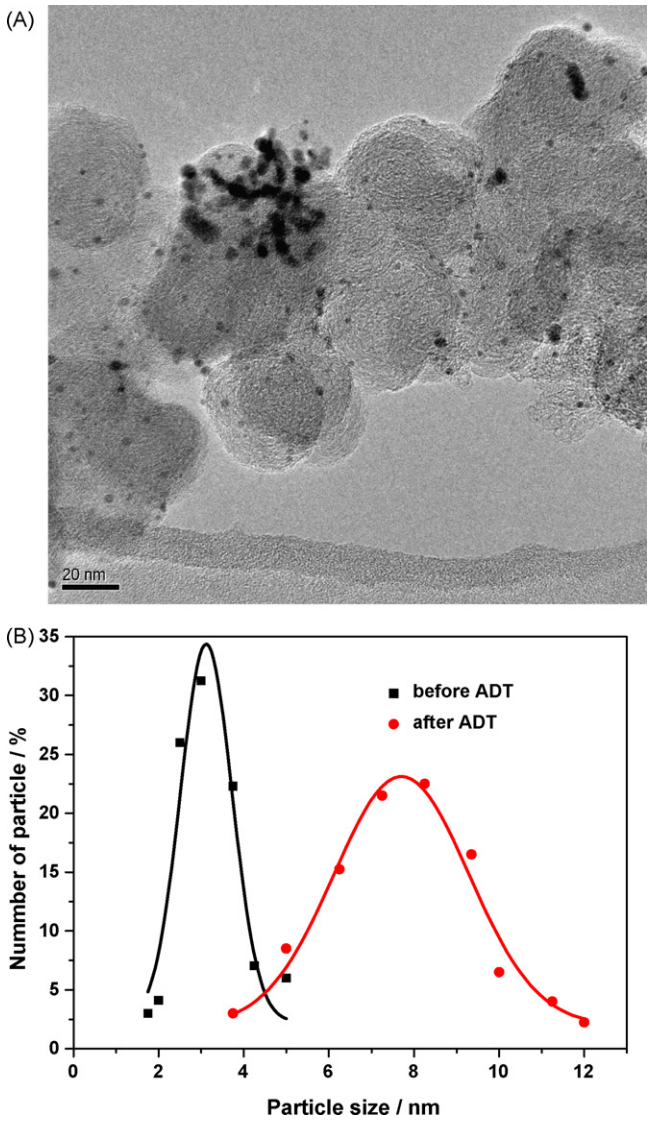

Fig. 6. HRTEM image of the commercial 20 wt.% Pt/C catalyst after ADT (A); particle size distribution of Pt before and after ADT (B).

mercial Pt/C catalyst shows a remarkable 160 mV degradation in half-wave potential after the ADT due to the carbon corrosion and subsequent catalyst particles dissolution and agglomeration. In contrast, the corresponding shift of the Pt/SiC/C catalyst is only 127 mV because there is not a significant degradation of the ECSA during potential cycling. As expected, the change of ORR activities is remarkably consistent with the ECSA loss as mentioned above.

Figs. 6 and 7 show an occurrence of agglomerations of Pt nanoparticles in both Pt/C and Pt/SiC/C catalysts after ADT. Meanwhile the histogram of the particle size distribution of Pt is plotted, which is obtained from several random areas in the HRTEM images containing about 200 particles. In the case of the Pt/C catalyst, Pt particles agglomerate on the carbon supports after ADT, leading to a massive decrease of Pt particles and leaving behind more bare carbon surfaces as shown in Fig. 6A, where the average particle size increases from 3 to 8 nm (Fig. 6B). In contrast, slight agglomeration of Pt particles is observed for the Pt/SiC/C, there is still a large number of Pt particles remaining on the ceramic surfaces (Fig. 7A and B) with only a small increase in the average particle size from 3 to 6 nm (Fig. 7C). Thus, the Pt/C catalyst displays a faster agglomeration of Pt particles than the Pt/SiC/C, which demonstrates a higher

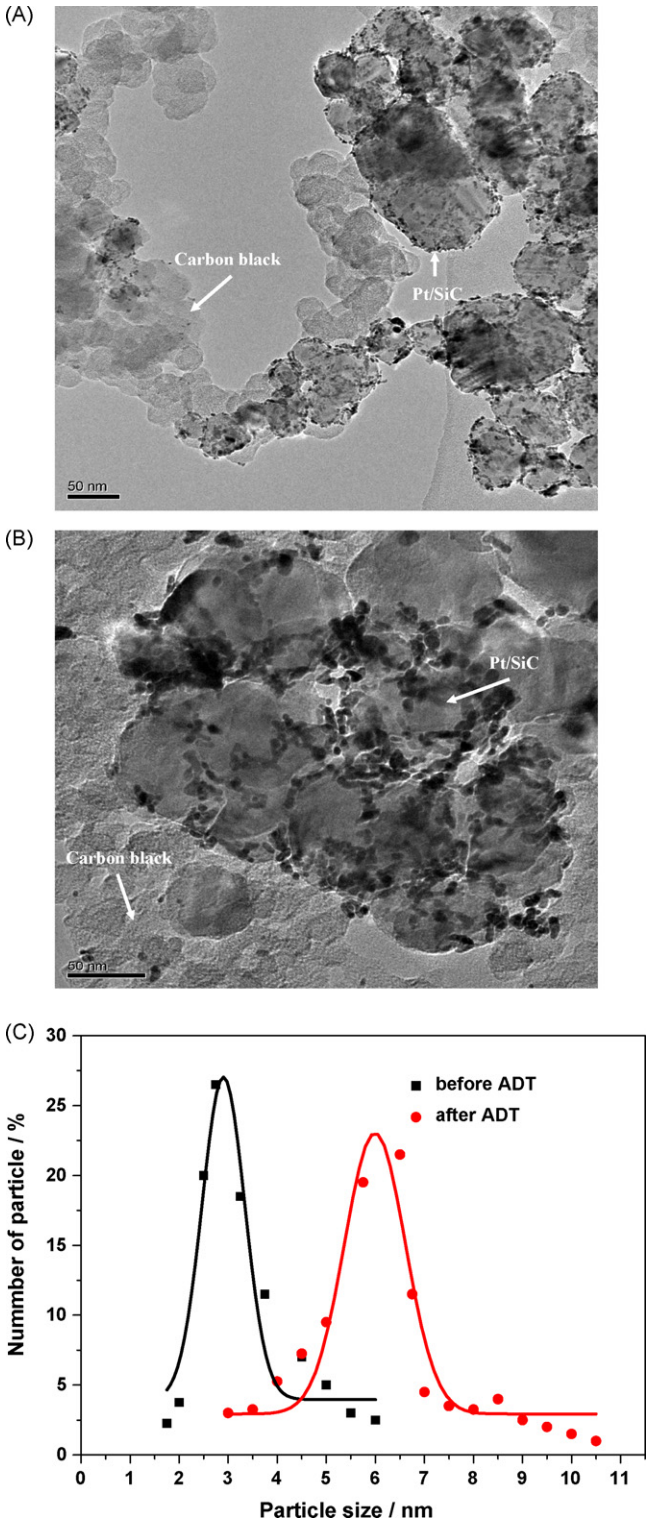

Fig. 7. HRTEM images of the as-prepared Pt/SiC/C catalyst before ADT (A) and after ADT (B); particle size distribution of Pt before and after ADT (C).

electrochemical stability of Pt/SiC/C in comparison with Pt/C. It is important to note that the dissolution and aggregation of nanoparticles occur to both the Pt/SiC/C and Pt/C catalysts, which may be the main reason of Pt particle size increase.

Both the ADT and TEM results indicate that the selective SiC support material promote the stabilization of Pt catalysts. The Pt particle size in both commercial Pt/C and Pt/SiC/C catalysts is in the

range of 2–5 nm, which endows Pt particles with a strong tendency to agglomeration. In fact, carbon supports in fuel cell cathodes can be oxidized to CO_2 or CO in the case of fuel starvation, and can be promoted in the presence of Pt [17,22], accelerating the agglomeration of Pt particles. In contrast, the SiC supports have much higher corrosion resistance than carbon supports, therefore the interaction between Pt particles and the SiC support is enhanced and decreases the agglomeration of Pt particles. The addition of carbon enhances the catalytic activity and electrochemical stability of Pt/SiC/C by improving the electrical conductivity of the Pt/SiC catalysts. Meanwhile, it is noteworthy that the carbon in Pt/SiC/C is bare and has no Pt deposition on its surface (Fig. 7A and B). It is more stable than the Pt-deposited carbon in Pt/C catalysts because of the faradic reactions between Pt nanoparticles and supports, which could accelerate the oxidation of carbon [23].

4. Conclusion

In this study, homogeneously dispersed Pt nanoparticles were successfully deposited on β-SiC (Pt/SiC) using an ethylene glycol reduction method. To further improve the electrocatalytic activity and electrochemical stability of Pt/SiC catalysts, the Pt/SiC/C catalyst was obtained by introducing Vulcan XC-72 into the Pt/SiC. The HRTEM images revealed that Pt nanoparticles homogeneously disperse on SiC with a particle size of ∼3 nm. The prepared Pt/SiC/C catalyst is almost identical in ORR activity with the conventional Pt/C catalysts. Most notably, the stability of Pt/SiC/C is more enhanced than the Pt/C. These results show that the Pt/SiC/C is a promising catalyst for PEM fuel cell applications. Furthermore, the ECSA of this catalyst can be further enhanced by using advanced nano-carbon materials or optimizing the proportion of carbon and Pt/SiC. Also, the addition of carbon in a ceramic supported catalyst supplies a possibility to prepare an advanced catalyst with high electrocatalytic performance and stability by using nano-ceramic materials as supports with relatively low or non-electrical conductivity. This additional research is in progress.

Acknowledgments

This work was supported by the New Century Excellent Talent Program of Ministry of Education of China (NCET-07-0652), the National Science Foundation of China (50972112, 50632050), the Fundamental Research Funds for the Central Universities, and the Self-determined and Innovative Research Funds of WUT.

References

[1] J. Zhang, K. Sasaki, E. Sutter, R.R. Adzic, Science 315 (2007) 220–222.
[2] H.R. Colon-Mercado, B.N. Popov, J. Power Sources 155 (2006) 253–263.
[3] Y.G. Chen, J.J. Wang, H. Liu, R.Y. Li, X.L. Sun, S.Y. Ye, S. Knights, Electrochem. Commun. 11 (2009) 2071–2076.
[4] N.C. Cheng, S.C. Mu, M. Pan, P.P. Edwards, Electrochem. Commun. 11 (2009) 1610–1614.
[5] L.M. Roen, C.H. Paik, T.D. Jarvi, Electrochem. Solid-State Lett. 7 (2004) A19–A22.
[6] D.A. Stevens, J.R. Dahn, Carbon 43 (2005) 179–188.
[7] B. Avasarala, T. Murray, W.Z. Li, P. Haldar, J. Mater. Chem. 19 (2009) 1803–1805.
[8] S.B. Yin, S.C. Mu, H.F. Lv, N.C. Cheng, M. Pan, Z.Y. Fu, Appl. Catal. B 93 (2010) 233–240.
[9] S.Y. Huang, P. Ganesan, S. Park, B.N. Popov, J. Am. Chem. Soc. 131 (2009) 13898–13899.
[10] T. Narushima, T. Goto, T. Hirai, J. Am. Ceram. Soc. 72 (1989) 1386–1390.
[11] J.C. Summers, S. Van Houtte, D. Psaras, Appl. Catal. B 10 (1996) 139–156.
[12] M.J. Ledoux, F. Meunier, B. Heinrich, C. Pham-Huu, M.E. Harlin, A.O.I. Krause, Appl. Catal. A 181 (1999) 157–170.
[13] J.J. Wang, G.P. Yin, Y.Y. Shao, S. Zhang, Z.B. Wang, Y.Z. Gao, J. Power Sources 171 (2007) 331–339.
[14] F. Maillard, M. Martin, F. Gloaguen, J.M. Leger, Electrochim. Acta 47 (2002) 3431–3440.
[15] Z.L. Liu, L.M. Gan, L. Hong, W.X. Chen, J.Y. Lee, J. Power Sources 139 (2005) 73–78.
[16] E. Antolini, L. Giorgi, F. Cardellini, E. Passalacqua, J. Solid State Electrochem. 5 (2001) 131–140.
[17] S.D. Knights, K.M. Colbow, J. St-Pierre, D.P. Wilkinson, J. Power Sources 127 (2004) 127–134.
[18] J.S. Ye, X. Liu, H.F. Cui, W.D. Zhang, F.S. Sheu, T.M. Lim, Electrochem. Commun. 7 (2005) 249–255.
[19] L. Lauermann, R. Memming, D. Meissner, J. Electrochem. Soc. 144 (1997) 73–80.
[20] Y.H. Zhang, M.L. Toebes, A. van der Eerden, W.E. O'Grady, K.P. de Jong, D.C. Koningsberger, J. Phys. Chem. B108 (2004) 18509–18519.
[21] J. Nicole, D. Tsiplakides, C. Pliangos, X.E. Verykios, C. Comninellis, C.G. Vayenas, J. Catal. 204 (2001) 23–34.
[22] L.M. Roen, C.T. Paik, D.H. Jarvi, Electrochem. Solid State Lett. 7 (2004) A19–A22.
[23] L. Li, Y.C. Xing, J. Electrochem. Soc. 153 (2006) A1823–A1828.